

Experimental and Theoretical Investigation of the Pyrrole/Al(100) Interface[†]

Alessandro Ruocco,^{*,‡} Letizia Chiodo,[§] Massimo Sforzini,^{||} Maurizia Palumbo,[⊥]
Patrizia Monachesi,[#] and Giovanni Stefani[‡]

Dipartimento di Fisica and CNISM Università Roma Tre, Roma, Italy, Nano-Bio Spectroscopy group and European Theoretical Spectroscopy Facility (ETSF), Dpto. de Física de Materiales, Universidad del País Vasco UPV/EHU and Centro Mixto CSIC-UPV/EHU, San Sebastián, Spain, Dipartimento di Fisica Università Roma Tre, Roma Italy, Dipartimento di Fisica, European Theoretical Spectroscopy Facility (ETSF), CNR-INFN-SMC, Università di Roma "Tor Vergata", Roma, Italy, and Dipartimento di Fisica, Università de L'Aquila, L'Aquila, Italy

Received: June 12, 2009; Revised Manuscript Received: October 8, 2009

The electronic properties of the pyrrole/Al(100) interface have been investigated from both a theoretical and experimental point of view. Electron energy loss spectroscopy (EELS) in specular reflection geometry does not reveal modification of the electronic structure of the molecule when adsorbed on the Al surface. EELS results and the low desorption temperature of pyrrole indicate a weak molecule/metal interaction. Ab initio calculations in the framework of the single-particle density functional theory within the local density approximation was used to investigate the adsorption energy and geometry. The low adsorption energy, -0.51 eV per molecule, and the high N–Al distance, 1.98 Å, confirm the weak interaction of pyrrole adsorbed on the Al surface.

Introduction

The pyrrole molecule (C_4H_5N , a five-atom aromatic ring with six π electrons) is a fundamental building block for biological systems, such as chlorophyll and hemoglobin. The pyrrole ring is also present in natural colored products, such as porphyrins and phthalocyanines. The molecule and its derivatives are used in synthesis of pharmaceuticals, dyes, photographic chemicals, and other organic compounds. It also finds technological applications as catalyst for polymerization process and corrosion inhibitor. Beyond the technological applications of the molecule per se, there is interest in pyrrole as a component of organic–inorganic interfaces. One of the fields in which these interfaces are becoming of dominant interest is, for example, the hybrid photovoltaics, which aim at finding systems that combine good photon absorption with good capability of injecting charge into the inorganic semiconductor.¹ Furthermore, microelectronic industry makes use of a thin film of conductive polymer for the realization of new devices. A good candidate, due to its high conductivity, is the polypyrrole.² In this context, understanding the formation of the pyrrole/Si interface is fundamental to the preparation and manipulation of thin film based on such interface. Qiao et al.^{3,4} made evident the formation of covalent bonding between pyrrole and the Si(100) surface via dissociation of N–H bonding and successive formation of N–Si bond. This result has been confirmed by further experiment⁵ and theory.⁶

Less is known on the pyrrole/metal interfaces. The chemisorption and decomposition of pyrrole on the Pd(111) surface⁷

was studied for its importance in catalysis of organic molecules. At variance with other interfaces, the pyrrole/Cu(100)⁸ interface does not show evidence for chemisorption or dissociation of the adsorbed molecule and the interaction is driven by the molecular π orbital.

This work is devoted to study, both theoretically and experimentally, the formation and the fundamental properties of the pyrrole/Al(100) interface. Al was chosen as a prototype of a simple sp metal in contrast with the transition metal where the d band is strongly involved in the bonding mechanism. Al is also technologically relevant as a contact material in organic electronic devices.

The computational analysis of the adsorption mechanism of pyrrole on Al(001) is focused on a selection of possible adsorption geometries among which we test the most stable configuration and calculate the electronic properties of the hybrid pyrrole/Al(001) system. The results are compared with the experimental energy loss spectra of pyrrole/Al interfaces grown in situ with different molecular exposure.

Experimental Section

The energy loss spectra, taken with an incident current of the order of 1 nA, have been measured in specular reflection geometry with an incidence angle of 30° and a primary energy of 140 eV. This energy corresponds to a minimum of the elastic I/V curve of the clean Al(100) surface, and it was chosen to increase the sensitivity to the overlayer. The surface was oriented with the [011] direction in the scattering plane. The overall energy resolution of 0.6 eV is obtained with the electron analyzer working in fixed pass energy mode and with an angular resolution of 1° . Details of the experimental chamber and of the analyzer are given elsewhere.⁹ The clean Al(100) surface was prepared by Ar^+ sputtering (3 keV) and annealing (400 °C). Pyrrole was introduced in the preparation chamber through a leak valve, the sample was exposed to a pyrrole pressure, at room temperature, between 5×10^{-8} and 5×10^{-7} mbar. The

[†] Part of the "Vincenzo Aquilanti Festschrift".

* To whom correspondence should be addressed. E-mail: ruocco@fis.uniroma3.it.

[‡] Dipartimento di Fisica and CNISM, Università Roma Tre.

[§] Universidad del País Vasco UPV/EHU and Centro Mixto CSIC-UPV/EHU.

^{||} Dipartimento di Fisica, Università Roma Tre.

[⊥] Università di Roma "Tor Vergata",

[#] Dipartimento di Fisica, Università de L'Aquila.

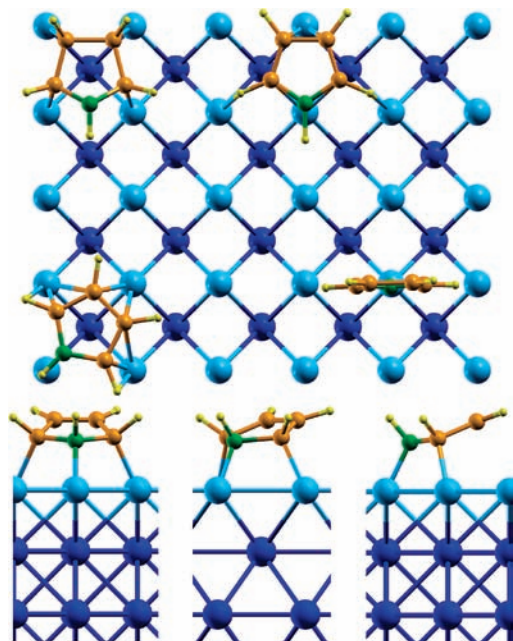


Figure 1. Top panel: adsorption geometries of pyrrole on Al(100): *hol0* (top left), *hol45* (bottom left), *bri0* (top right), *top0* upright (bottom right). Bottom panel, from left to right: most stable adsorption geometry, *hol45*, viewed from different orientations. Color key: light blue, the Al atoms belonging to the surface; blue, the atoms in the bulk.

total exposure ranges between 180 and 2030 langmuir (1 langmuir = $1 \text{ s} \times 1 \times 10^{-6} \text{ mbar}$). The cleanliness of the Al surface was verified by monitoring the Al $L_{2,3}VV$ Auger transition.

Theoretical Methodology

The theoretical results presented here are obtained performing ab initio calculations in the framework of the single-particle density functional theory within the local density approximation (DFT-LDA) for the exchange-correlation potential (in the Perdew–Zunger parametrization), as implemented in the Quantum-ESPRESSO package.¹⁰ Norm-conserving Trouiller–Martins pseudopotentials have been used for all the atoms. To simulate the Al(100) surface, clean and with adsorbed pyrrole, we used the repeated slab approach with periodic boundary conditions. To avoid the interaction between neighboring slabs, the supercell is chosen to be large enough (with more than 20 Å of vacuum) perpendicularly to the surface plane. The hybrid interface is represented by a five-layer slab, with a 2×2 and 3×3 surface cell. The optimization of adsorption structure for the various configurations (see Figure 1) has been performed with the smaller cell, while the larger surface cell has been used to find the most stable geometry in the calculations that follow. The 3×3 cell dimensions is $8.51 \text{ Å} \times 8.51 \text{ Å}$, which, compared to the molecule lateral dimension of about 4.5 Å, is large enough to avoid lateral interaction between molecules located in neighboring cells. The atomic slab geometries have been relaxed with the direct energy minimization technique of Broyden–Fletcher–Goldfarb–Shanno,¹⁰ and the forces on each atom have been converged to 0.0025 Ry/a.u. An energy cutoff of 50 Ry and sampling of Monkst–Pack k points have been used to integrate over the Brillouin zone, with the number of k points varying according to the supercell dimension, from 3 to 10 in the irreducible Brillouin zone.

We have carefully checked the convergence of the relevant quantities (e.g., adsorption energy, density of states) with respect to the calculation parameters, as k -points and energy cutoff.

TABLE 1: Bond Lengths (Å) and Angles (deg) for the Free Pyrrole and Their Variations Induced by the Adsorption on the Al(100) Surface

	free pyrrole	adsorbed pyrrole
N–C ₁	1.36	1.51
C ₁ –C ₂	1.37	1.47
C ₂ –C ₂	1.41	1.35
N–H	1.01	1.02
C ₁ –H	1.09	1.11
C ₁ –H	1.09	1.09
C ₁ NC ₂	110.0	106.5
C ₂ C ₁ N	108.0	103.5
C ₁ C ₂ C ₂	107.0	101.4

Adsorption of Pyrrole on Al(100)

Pyrrole Geometry Adsorption. Structural, electronic, and optical properties of an isolated pyrrole molecule has been presented elsewhere.¹¹ Here, various starting configurations of the pyrrole molecule adsorbed on the Al surface, with the pyrrole in both planar and upright geometry, have been investigated. The adsorption energy for the single molecule on the surface is calculated as

$$E_{\text{ads}} = E_{\text{pyrr/Al}}^{\text{slab}} - E_{\text{Al}}^{\text{slab}} - E_{\text{pyrr}} \quad (1)$$

With this definition, adsorption occurs if $E_{\text{ads}} < 0$.

We considered the planar geometries reported in 1: *hol0* ($E_{\text{ads}} = -0.41 \text{ eV}$), in which the molecule adsorbs with its geometrical “center of mass” corresponding to a hollow site of the surface and the nitrogen atom along the [100] direction; *hol45* ($E_{\text{ads}} = -0.51 \text{ eV}$), in the same position but rotated by 45° with respect to the *hol0*; and *bri0* ($E_{\text{ads}} = -0.09 \text{ eV}$), with the molecule “center of mass” in a bridge site, but not rotated. Various other planar configurations, plus an upright configuration, *top0*, have been tested, but they have lower adsorption energies, or they are even unstable, giving rise to systems not bound to the metal surface.

Thus, the most favorable adsorption geometry, the *hol45*, corresponds to the nitrogen atom directly placed above an aluminum atom. This indicates an interaction probably driven by the electron pair contributed by nitrogen. However, as shown in the following density of states analysis, also carbon atoms participate, to a certain extent, to the bonding. The molecule–substrate interaction induces a deformation of the original planar geometry (see Figure 1): in particular, hydrogen atoms are tilted away from the surface. Variations of bond lengths and angles, due to adsorption, with respect to the free molecule, are reported in Table 1.

The nature of the interaction between the molecule and metal surface is now analyzed. The considerations that follow concern the structure and the energy of the pyrrole/Al(100) interface. They are based on electronic structure calculations performed in the density functional theory (DFT) characterized by the local description of the exchange–correlation functionals. The N–Al distance, found to be 1.98 Å, can be interpreted as the first clue that pyrrole is physisorbed on the Al surface since chemisorption bonds are usually shorter. For comparison, Seino et al. have obtained in the chemisorption of pyrrole on Si(100) a N–Si distance of 1.76 Å.⁶ Physisorption of pyrrole on the Al surface is further suggested by the low adsorption energy (-0.51 eV). The simultaneous occurrence of a large bond length and of a low adsorption energy, also found in other aromatic molecules on Al substrates,^{12,13} strongly supports the picture of a phys-



Figure 2. $\Delta\rho(\mathbf{r})$, for isosurface values (from left toward right) ± 0.06 , ± 0.04 , and ± 0.02 $e/\text{\AA}^3$. Electron accumulation $\Delta\rho(\mathbf{r}) > 0$ is displayed in red; electron depletion $\Delta\rho(\mathbf{r}) < 0$ in blue.

isorption process that does not involve a direct covalent bond, but rather an interaction between mutual polarizations due to the van der Waals force. This weak, strictly nonlocal interaction between adsorbate and substrate leads to an adsorption energy typically less than -0.3 eV per particle.¹⁴ van der Waals interaction is missed in the DFT description of the local-density approximation (LDA) and of the generalized gradient approximation (GGA) for the DFT exchange–correlation functionals. Therefore, the quantitative determination of adsorption energy and bond length in DFT must be taken with care for calculated binding energies close to -0.3 eV, typical of van der Waals energy. The bond length and adsorption energy of pyrrole on aluminum can be compared with the values obtained for the adsorption of a larger organic molecule, adenine, on Cu(110):¹⁵ the Cu–N distance is 2.32 Å, and the adsorption energy -0.34 eV. Even if van der Waals forces are not taken into account in this kind of ab initio calculation, a physisorption process has been assumed for adenine. In our case, however, a shorter Al–N distance and a slightly higher binding energy seems to indicate a stronger bond than in the adenine case. The pyrrole–aluminum interaction seems to be more intense than a bare physisorption process. Finally, on the Si(001) surface, stable configurations are realized through the N–H bond dissociation, and the subsequent bonding between N and Si of covalent character. Such dissociative configurations seem, however, to be unstable on Al(100).

A practical way to visualize the formation and character of the bonding is the charge density difference, as a function of position \mathbf{r} , $\Delta\rho(\mathbf{r}) = \rho_{\text{Al}}(\mathbf{r}) + \rho_{\text{pyr}}(\mathbf{r}) - \rho_{\text{pyr}/\text{Al}}(\mathbf{r})$, where $\rho_{\text{pyr}/\text{Al}}$ is the total electron density of the relaxed adsorbate/substrate system, ρ_{Al} is the density of the relaxed clean aluminum slab, and ρ_{pyr} is that for an isolated pyrrole molecule. To obtain the quantity $\Delta\rho(\mathbf{r})$, the supercells for the three different systems have been constructed with the same dimensions, energy cutoff, and number of k -points. The charge density behavior seems to suggest, for pyrrole/Al, a situation different from the bond between adenine and copper.¹⁵ In Figure 2 the total charge density difference is reported, with the region of electron accumulation displayed in red, and the region of electron depletion in blue. The isosurface values are respectively ± 0.06 , ± 0.04 , and ± 0.02 $e/\text{\AA}^3$. The charge density difference plot clearly shows the occurrence of electron accumulation along the bond direction of N–Al and C_1 –Al, where C_1 denotes neighboring carbon atoms of nitrogen (C_2 denotes C atoms farther from nitrogen). The electron depletion appears delocalized on the surface aluminum layer. Comparison with adenine/Cu(110)¹⁵ further confirms the differences already observed in bond lengths and adsorption energy. In fact, for adenine, a true polarization is observed in the space between metal and molecule, while in the present case there is an electron accumulation between pyrrole and Al.

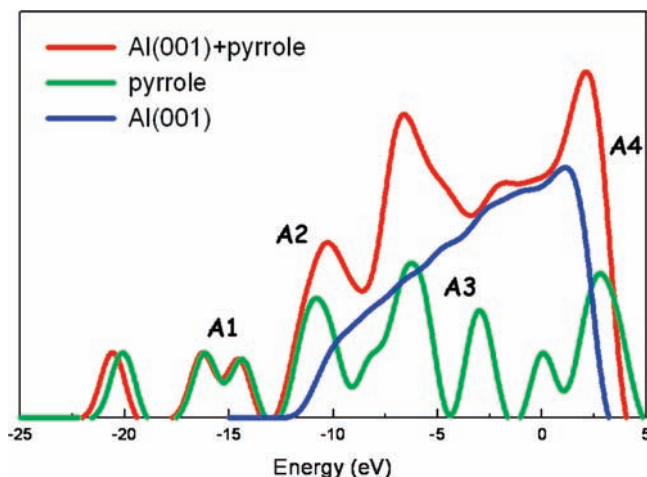


Figure 3. Density of states of the three systems: pyrrole, Al(001) surface, and pyrrole/Al(001). The features denoted by A_i are described in the text. The zero of the energy scale corresponds to the Fermi level.

Density of State. The nature of interaction between molecule and metal surface is also confirmed by the analysis of the density of states (DOS). At variance with what is observed for the case of covalent bonds between adsorbates and substrate,^{16–19} where the metal states are strongly affected by the interaction with the organic molecules and the bond formation is clearly ascribable to the presence of new hybrid states, here we observe that the DOS of the overall system is given by the sum of the two individual systems, with only slight variations induced by the interaction.

In particular, from the analysis per atom and per orbital component of the density of states, performed by the FPLMTO method (see refs 16, 18, and 20 for further details) we characterized the nature of the individual DOS peaks, reported in Figure 3. The peak A1 is given by s-orbitals from C_1 – C_2 atoms of the pyrrole. Both N p-states and C_1 – C_2 s-states contribute to the structure A2. The peak A3 has p nature, from both N and C_1 atoms, and finally, the structure A4 is due to p-orbitals from N. A very low hybridization is thus observed between the molecular states and the Aluminum sp-states.

Experimental Results

In Figure 4 several EELS spectra measured as a function of the pyrrole exposure ranging from 180 to 2030 langmuirs are reported. For comparison the clean Al spectrum is also reported. This latter spectrum is dominated by two intense peaks corresponding to the excitation of the surface (10.2 eV) and bulk (15 eV) plasmons. The EELS spectrum is not clearly modified after an exposure of 180 and 340 langmuirs. The first modifications start after 600 langmuirs of pyrrole. In particular

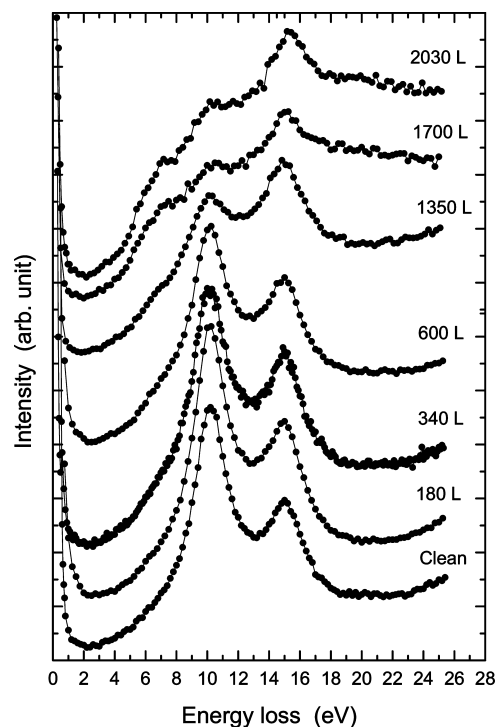


Figure 4. EEL spectra of the Al(100) surface as a function of the exposure to pyrrole. The primary energy is 140 eV.

the surface plasmon is slightly depressed, the valley between the two plasmon is shallower and a new structure around 7 eV appears. For exposure in excess of 1350 langmuirs of pyrrole, the surface plasmon intensity continues to decrease while the structure around 7 eV becomes more evident. This trend continues up to 1700 langmuirs while the spectra at 1700 and 2030 langmuirs are very similar, indicating that a saturation condition was reached. In particular, taking into account the fact that the surface and bulk plasmon are attenuated but still visible, the saturation could correspond to the completion of a pyrrole monolayer. This result is not surprising considering that the sample was kept at room temperature during the exposure to pyrrole. A desorption temperature of pyrrole layers not directly bonded to the substrate of 165 and 170 K were found in the case of pyrrole/Cu(100)⁸ and pyrrole/Pd(111)⁷ interfaces. Then, the formation of a multilayer at room temperature is practically forbidden as a consequence of the low pyrrole–pyrrole interaction. In the case of pyrrole/Si interface³ an exposure to 4 langmuirs was enough for the formation of the first half layer, in our case the saturation in EELS spectra is reached after 1700 langmuirs. This is a clear indication that the sticking coefficient is small as a consequence of the weak pyrrole/Al interaction.

To better understand the modification of the EEL spectrum after the exposure of the Al(100) surface to pyrrole, we have analyzed the spectrum at 2030 langmuirs by means of a fitting procedure. The best fit is obtained with a trial function made of two Voigt profiles to simulate Al plasmons and five other ones to reproduce the main molecular absorption bands observed in gaseous pyrrole by VUV^{21,22} and EEL spectroscopies.²³ The result of a χ^2 minimization is reported in Figure 5. In particular, we observe components in the fit at 6.0, 7.3, 9.2, 12.7, and 17.4 eV. The first two components at 6.0 and 7.3 eV find a counterpart in the EELS spectrum of the pyrrole in gas phase²³ that is dominated by a sharp peak centered at 6 eV and a wider peak centered at 7.5 eV. The limited energy range of the gas phase spectrum (5–12 eV) does not allow for a direct comparison of features at higher energy. The mirror kinematics

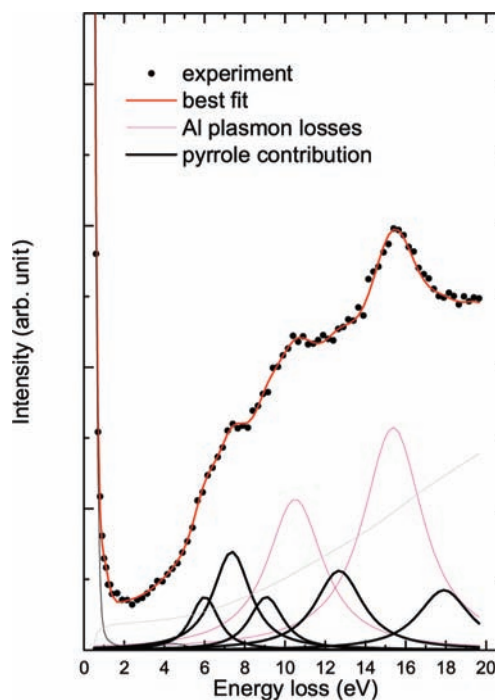


Figure 5. Best fit of the EEL spectrum taken after an exposure of the Al surface to 2030 langmuirs of pyrrole. The violet lines are the contribution from the Al surface and bulk plasmons; the black lines represent the contribution originating from pyrrole.

adopted for the experiment allows us to make use of the double collision model²⁴ that, together with the limited accepted solid angle of the analyzer, grants for validity of dipole approximation. It is therefore possible to compare present results with the VUV absorption spectra.^{21,22} In particular, the components in our spectrum at 17.4 eV find a counterpart in the bands centered at 17 eV of the VUV absorption spectra.²² The other two components obtained from the fit at 9.2 and 12.7 eV should correspond to the faint modulations present in the VUV spectrum.²² A complete discussion on the origin and symmetry of the transitions observed in the EEL and VUV absorption spectra is found in ref 21. The comparison with EEL and VUV absorption spectra in the gas phase does not reveal modification of the molecule adsorbed on the Al(100) surface suggesting, in agreement with the main theoretical results presented in the previous section, a weak interaction with the substrate.

In Figure 6 it is possible to observe that after annealing to 380 °C of Al surface exposed to 1700 langmuirs, the EEL spectrum is almost identical to one obtained on the clean Al surface prepared by sputtering and annealing. In particular the surface Al plasmon is again the dominant feature. These spectra suggest that after annealing the molecule is completely desorbed from the Al surface. During the annealing the products of thermal desorption were monitored by a mass spectrometer mounted in front of the sample; starting from a temperature of 260 °C the presence of a peak at 67 amu/e indicates that the molecule is desorbed entire. In the case of the pyrrole/Si interface the thermal desorption happens at much higher temperature (800 K) while in the mass spectrum is registered a peak at 66 amu/e reflecting the fact that it was chemically bound to the substrate after the cleavage of N–H bond and the creation of N–Si bond. The low desorption temperature observed for the pyrrole/Al system is a further evidence for the weakness of the molecule/substrate interaction with respect of the case of semiconductor substrates. Other aromatic molecules grown on the Al surface have similar or even weaker interactions. In the

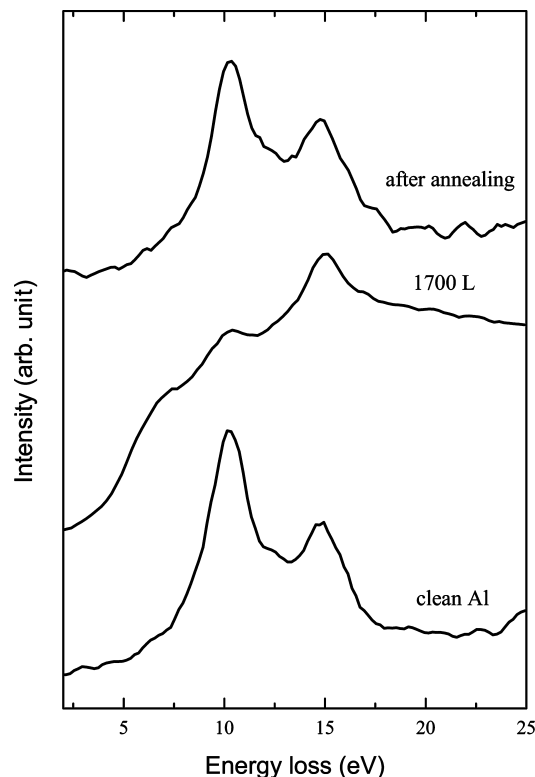


Figure 6. EEL spectra of the as prepared clean Al surface (bottom), after a pyrrole exposure of 1700 langmuirs with the substrate at room temperature (middle) and after the annealing of the sample up to 380 °C (top).

case of benzene grown on the Al(111) surface^{12,13} the thermal desorption of the first and successive molecular multilayer is indistinguishable, the first layer desorbs at 150 K, a much lower temperature with respect to the 260 °C of the pyrrole/Al case.

Conclusions

Although experimental data and calculations are not directly comparable, they both support the model of a weak interaction between pyrrole and the Al substrate. In fact, the energy loss spectrum can be considered, in a simplified picture, as the superposition of the clean Al surface and of the isolated molecule spectrum; also the calculated DOS can be viewed as the sum of the DOS of the substrate and of the molecule. The weak interaction is confirmed by the calculated binding energy (−0.51 eV) and by the observed desorption temperature (260 °C). The charge density analysis indicates a charge redistribution between molecule and metal, with electron accumulation mainly between the pyrrole and the metallic substrate, and electron

depletion in the molecular plane. This behavior, which differs from previously reported organic–metal systems,¹⁵ could be the origin for an interaction slightly stronger than a mere physisorption.

Acknowledgment. M.P. and L.C. acknowledge funding by the European Community through e-I3 ETSF project (INFRA-2007-1.2.2: Grant Agreement Number 211956), the CINECA Supercomputing Center through CNR-INFM projects (accounts cne0fm2v), and the Barcelona Supercomputing Center, Red Espanola de Supercomputacion. L.C. acknowledges the Universidad del País Vasco UPV/EHU. This work was partially funded by MIUR (PRIN 2003028141).

References and Notes

- (1) Oregan, B.; Graetzel, M. *Nature* **1991**, *353*, 737.
- (2) Bätz, P.; Schmeisser, D.; Göpel, W. *Phys. Rev. B* **1991**, *43*, 9178.
- (3) Qiao, M. H.; Cao, Y.; Deng, J. F.; Xu, G. Q. *Chem. Phys. Lett.* **2000**, *325*, 508.
- (4) Qiao, M.-H.; Tao, F.; Cao, Y.; Xu, G.-Q. *Surf. Sci.* **2003**, *544*, 285.
- (5) Kim, K.-j.; Han, J.; Kang, T.-H.; Ihm, K.; Jeon, C.; Moon, S.; Hwang, C.-C.; Hwang, H.-N.; Kim, B. *J. Electron Spectrosc. Relat. Phenom.* **2005**, *144–147*, 429.
- (6) Seino, K.; Schmidt, W. G.; Furthmüller, J.; Bechstedt, F. *Surf. Sci.* **2003**, *532–535*, 988.
- (7) Baddeley, C. J.; Hardacre, C.; Ormerod, R. M.; Lambert, R. M. *Surf. Sci.* **1996**, *369*, 1.
- (8) Sexton, B. A. *Surf. Sci.* **1985**, *163*, 99.
- (9) Ruocco, A.; Donzello, M. P.; Evangelista, F.; Stefani, G. *Phys. Rev. B* **2003**, *67*, 155408.
- (10) Baroni, S.; Dal Corso, A.; de Gironcoli, S.; Giannozzi, P. <http://www.pwscf.org/>, 2001.
- (11) Chiodo, L.; Bruno, M.; Palumbo, M.; Monachesi, P. *Phys. Status Solidi (b)* **2005**, *242*, 3032.
- (12) Blomqvist, J.; Salo, P. *J. Phys.: Condens. Matter* **2009**, *21*, 225001.
- (13) Duschek, R.; Mittendorfer, F.; Blyth, R. I. R.; Netzer, F. P.; Hafner, J.; Ramsey, M. G. *Chem. Phys. Lett.* **2000**, *318*, 43.
- (14) Scheffler, M.; Stampfl, C. *Theory of Adsorption on Metal Substrates*; Elsevier: Amsterdam, 1999.
- (15) Preuss, M.; Schmidt, W. G.; Bechstedt, F. *Phys. Rev. Lett.* **2005**, *94*, 236102.
- (16) Monachesi, P.; Palumbo, M.; Del Sole, R.; Grechnev, A.; Eriksson, O. *Phys. Rev. B* **2003**, *68*, 035426.
- (17) Monachesi, P.; Chiodo, L.; Del Sole, R. *Phys. Rev. B* **2004**, *69*, 165404.
- (18) Chiodo, L.; Monachesi, P. *Phys. Rev. B* **2007**, *75*, 075404.
- (19) D'Agostino, S.; Chiodo, L.; Della Sala, F.; Cingolani, R.; Rinaldi, R. *Phys. Rev. B* **2007**, *75*, 195444.
- (20) Baldacchini, C.; Chiodo, L.; Allegretti, F.; Mariani, C.; Betti, M. G.; Monachesi, P.; Del Sole, R. *Phys. Rev. B* **2003**, *68*, 195109.
- (21) Palmer, M. H.; Walker, I. C.; Guest, M. F. *Chem. Phys.* **1998**, *238*, 179.
- (22) Rennie, E. E.; Johnson, C. A. F.; Parker, J. E.; Ferguson, R.; Holland, D. M. P.; Shaw, D. A. *Chem. Phys.* **1999**, *250*, 217.
- (23) Flicker, W. M.; Mosher, O. A.; Kuppermann, A. *J. Chem. Phys.* **1976**, *64*, 1315.
- (24) Ruocco, A.; Milani, M.; Nannarone, S.; Stefani, G. *Phys. Rev. B* **1999**, *59*, 13359.

JP905537G